Peer-reviewed version available at *Journal of Human Genetics* **2020**; doi:10.1038/s10038-020-0819-6

Article

Identification of epigenetic interactions between microRNA and DNA methylation associated with polycystic ovarian syndrome

Zhanrui Mao [1], Ting Li [2], Hui Zhao [1], Yulan Qin [1] and Yani Kang [1,*]

[1] School of Biomedical Engineering, Bio-ID Center, Shanghai Jiao Tong University, Shanghai, 200240, China; maozhanrui@sjtu.edu.cn (Z.M.); zhaohuizh@sjtu.edu.cn (H.Z.); QinYulan10@sjtu.edu.cn (Y.Q.)

[2] Department of Obstetrics and Gynecology, Yuncheng Central Hospital, Yuncheng, 044000, Shanxi Province, China; 373714671@qq.com (T.L.)

* Correspondence: kangyani@sjtu.edu.cn; Tel.: +86 21 34207324

Abstract: Aberration in microRNA (miRNA) expression or DNA methylation is a causal factor for polycystic ovarian syndrome (PCOS), a common endocrine disorder and leading cause of infertility. However, the epigenetic interactions between miRNA and DNA methylation remain unexplored in PCOS. In this study, we conducted an integrated analysis of RNA-seq, miRNA-seq and MBD-seq on ovarian granulosa cells of PCOS and control groups to reveal the epigenetic interactions involved in the pathogenesis of PCOS. Firstly, we identified 830 genes and 30 miRNAs that were expressed differently in PCOS, and seven miRNAs were found to negatively regulate targeted mRNA expression. Next, in total, 130 miRNAs were found to be significantly differently methylated in promoter regions, while 13 were found to be associated with miRNA expression. Furthermore, the promoter hypermethylation of miR-429, miR-141-3p, and miR-126-3p was proven to suppress miRNA expression and therefore upregulate their corresponding genes, including *XIAP*, *BRD3*, *MAPK14* and *SLC7A5*. Our results demonstrate that DNA methylation regulates miRNA expression and therefore controls its corresponding gene expression. The reactivation of the transcription of epigenetically silenced genes may be one of the key elements in PCOS pathogenesis. Meanwhile, the epigenetic mechanisms underlying the regulation of miRNA expression can provide a potential therapeutic target for PCOS in the future.

Keywords: polycystic ovarian syndrome; granulosa cells; microRNA regulation; DNA methylation; biomarker;

1. Introduction

Polycystic ovarian syndrome (PCOS) is one of the most prevalent endocrine disorders with the symptoms of hyperandrogenism, chronic anovulation, and polycystic ovaries [1]. It is also considered to be a common cause of body malfunction in women, with symptoms including hirsutism, acne, obesity, menstrual dysfunction, and infertility. It also appears to be associated with an increased risk of metabolic aberrations, including insulin resistance and hyperinsulinism, type 2 diabetes mellitus, dyslipidemia, cardiovascular disease, and endometrial carcinoma [2,3].

Ovarian granulosa cells (GCs) have been demonstrated to play a major role in deciding the fate of follicles. In the early stage of follicle development, oocyte apoptosis results in follicular atresia-induced ambient GC death, which results in molecules that are essential for oocyte development and maintenance as well as self-renewal by apoptotic processes [4,5]. Therefore, it is important to investigate the role of GCs in the pathogenesis of PCOS.

Current research has shown that the influence of multiple factors, including age, the environment/lifestyle, and the disease state environment, can modify the clinical presentation of PCOS via epigenetic modifications [6]. DNA methylation and microRNAs (miRNAs) are two main

epigenetic modifications in the regulation of gene expression. MiRNAs are small noncoding RNAs acting as post-transcriptional negative regulators of gene expression, which are involved in the regulation of various diseases such as diabetes, insulin resistance, inflammatory disease, and cancer. Meanwhile, aberrant DNA methylation manifests in both global genome stability preservation and in localized gene promoter changes, which influences the transcription of disease-causing genes [7].

Recently, compelling evidence has indicated the roles of DNA methylation and miRNAs in PCOS, respectively. Previous studies detected significant alteration in genome-wide DNA methylation and transcriptional patterns in human ovaries, GCs and the adipose tissue of PCOS involved in metabolic disturbances [8-10]. These studies indicated that DNA methylation may be responsible for the development of PCOS. Similarly, the altered miRNA expression detected in human adipose tissue, follicular fluid, GCs, serum and peripheral blood leukocytes has been found to be associated with PCOS by targeting specific molecules and modulating various hormone-related and apoptosis-related pathways [11,12].

Though the epigenetic regulation of miRNAs and DNA methylation are both widely explored, the interaction mechanism of miRNAs and DNA methylation remain undiscovered in PCOS. DNA methylation regulates miRNA transcription by hyper-/hypo-methylating the promoter regions of miRNAs. Meanwhile, miRNAs can regulate genome-wide DNA methylation patterns by directly targeting DNA methyltransferases and methylation-related critical proteins [13,14].

In this study, we identified differentially expressed genes and miRNA in GCs of PCOS patients by transcriptome and small RNA sequencing. Then the miRNA-gene networks were constructed to demonstrate their regulatory functions involved in biological processes and pathways. Additionally, DNA methylation levels of miRNA promoter region was determined by methylated DNA binding domain sequencing (MBD-seq). Furthermore, the correlations between differential miRNA expression and promoter methylation were analyzed. And the epigenetic interactions between miRNA and methylation associated with target gene expression in PCOS were identified and validated by qRT-PCR. Our results revealed the complex interaction between miRNA and DNA methylation in PCOS at mRNA level.

2. Materials and Methods

2.1 Patient information and clinical characteristics

Twenty-seven participants (14 PCOS and 13 control) for this study were recruited from Yuncheng center hospital. This study was approved by the Ethics Committees on Human Research of Yuncheng center hospital (Approve ID: KYLL2019073). The diagnosis of PCOS patients proceeded by achieving at least two of the Rotterdam ESHRE/ASRM (2003) criteria [15]. The control group were fertile women with male partners experiencing sterility or infertile women with tubal blockages who received in vitro fertilization (IVF) treatment and with normal menstrual cycles, no polycystic ovary morphology, no clinical signs of hyperandrogenism, and no history of endometriosis or other chronic diseases. All participants were non-related Han people age between 20 and 35 years old from the same geographical region, and all agreed to participate in this study and provided written informed consent. The clinical characteristics of all participants are shown in Table 1.

2.2 Isolation of GCs

All participants were injected with gonadotropin-releasing hormone agonist (GnRHa) at the beginning of the mid-luteal phase, followed by ultrasound and serum estradiol to monitor follicle size. When three or more follicles with an average diameter of 16 mm were present, 5000 to 10,000 IU of human chorionic gonadotropin (HCG) was injected into participants. After 36 hours, oocytes were collected under ultrasound guidance while GCs around oocytes were retrieved and washed twice with Dulbecco's improved Eagle medium after oocyte removal. After that, the isolated GC samples were quickly put into liquid nitrogen and preserved at –80 ℃.

2.3 Total RNA and genomic DNA extraction

TRIzol (Invitrogen, Waltham, Massachusetts, USA) was used to extract total RNA from GC samples following the manufacturer's protocol. The total RNA quantity was determined with Nanodrop 2000 (Thermo Scientific, Waltham, Massachusetts, USA) and quality was assessed by performing 1% agarose gel electrophoresis, stained using with 4S Red Plus Nucleic Acid Stain (Sango, Shanghai, China).

Genomic DNA from GCs of PCOS patients and normal women was isolated by using the QIAamp DNA Mini Kit (Qiagen, Hilden, Germany) as recommended by the manufacturer.

2.4 Transcriptome sequencing and data analysis

One microgram of total RNA was used to construct the RNA-seq libraries by the KAPA Stranded RNA-Seq Library Preparation Kit (KAPA Biosystem, Wilmington, Massachusetts, USA). The quality of libraries was assessed with Agilent 2100 Bioanalyzer (Agilent, United States).
Sequencing reads were aligned to the UCSC Human Genome Browser hg38 assembly with HISAT2 (version 2.0.5), after data preprocessing [16]. Stringtie (version 1.3.3) was then used to determine the read counts per gene based on Ensembl gene-level annotations from Gencode release 31 (GRCh38.p12) [17]. The final unnormalized counts were assembled into a count-matrix with R (version 3.6.0), and this served as an input for DESeq2 (version 1.24.0) and edgeR (version 3.26.5) [18, 19]. In this study, the intersections of differentially expressed genes (DEGs) identified by DESeq2 and edgeR were used for further analysis, and expression changes with absolute value of $|\log_2$ fold changes$| \geq 1$ and p values < 0.05 were considered significant.

2.5 Small RNA sequencing and data analysis

One microgram of total RNA was used to construct the small RNA-seq libraries by the TruSeq® Small RNA Library Prep Kit (NEB, San Diego, California, USA) following the manufacturer's protocol. The quality of libraries was assessed with Agilent 2100 Bioanalyzer (Agilent, United States). Briefly, after trimming the adaptor sequences and filtering low-quality reads, all the clean reads were aligned against miRBase (version 22.1) using bowtie2 (version 2.1.0) [20,21]. Read counts were then calculated through a customized script. In this study, the intersections of differentially expressed miRNA (DEmiRs) identified by DESeq2 and edgeR were considered significant, and expression changes with absolute values of $|\log_2$ fold changes$| \geq 1$, RPM ≥ 0.1 and p values < 0.05 were considered significant. The target genes of DEmiRs were predicted with the miRTarbase database (Release 7.0) and used for further analysis [22]. Then, functional analysis was performed by clusterProfiler as mentioned above [23].

2.6 PPI network analysis of DEGs and DEmiRs

Based on target genes of the previously predicted DEmiRs, the protein-protein interaction network (PPI) network of DEG/DEmiR pairs was built with the STRING database (version 11.0) [24]. Cytoscape (version 3.6.0) was used to visualize the network [25].

2.7 MBD sequencing and bioinformatics analysis

Genomic DNA was fragmented with M220 Focused-ultrasonicator (Covaris, Woburn, Massachusetts, USA). The fragmented DNA with methylated CpGs (mCpG) were enriched using the MethylMiner™ Kit (Invitrogen, Waltham, Massachusetts, USA) as recommended by the manufacturer. The MBD-enriched fractions were used to generate indexed libraries with the NEBNext Ultra DNA Library Prep Kit for Illumina(NEB, San Diego, California, USA) as recommended by the manufacturer. The quality of libraries was assessed with Agilent 2100 Bioanalyzer (Agilent, United States).

MBD-seq raw data reads and filtered low-quality reads were mapped to the reference genome (Human hg38) using bowtie2 [20]. The MEDIPS analysis package (version 1.24.0) was used for the analysis and comparison of DNA methylation datasets of PCOS and controls [26]. P values <0.05 and $|\log_2$ fold changes$| \geq 1$ were considered to show differentially methylated regions. Raw sequence data

of MBD-seq were submitted to the GEO database and represented under one super-series along with transcriptome sequencing and small RNA sequencing data (Accession Number: GSE138575).

2.8 Methylation analysis of promoter region of miRNA associated with miRNA target gene expression

The transcription start site (TSS) data of DEmiRs were extracted from the FANTOM5 database, and 100 bp upstream and downstream were considered to be promoter regions of DEmiRs [27]. The identified differentially methylated miRNA promoter regions from the MBD-seq data were defined as differentially methylated promoters (DMPs).

2.9 Validation of the DEGs and DEmiRs expression by qRT-PCR

Five hundred nanograms of total RNA was used for reverse transcription by using the PrimeScript RT Master Mix (TAKARA), which contained a mixture of random 6-mers and oligo dT primer. Additionally, 500 ng of total RNA was used for reverse transcription using SuperScript II Reverse Transcription (Thermo Scientific, Waltham, Massachusetts, USA) with miRNA-specific stem loop primers. Quantitative real-time PCR (qRT-PCR) was then carried out with a PowerUp SYBR Green Master Mix (Applied biosystems) at the StepOne Plus qPCR instrument (Applied Biosystems). Primer sequences are shown in Table S1.

2.10 Statistical analysis

Statistical analyses were conducted by using Statistical Package for Social Sciences (SPSS) version 20.0 software (IBM Corp., Armonk, NY, USA). The differences between groups were assessed by a two-sided Student's t-test, and $p < 0.05$ was considered statistically significant.

3. Results

3.1. Comparison of clinical data between PCOS patients and normal women

The clinical data including age, height, weight, circumference and serum levels of seven sex hormones—follicle-stimulating hormone (FSH), estrogen (E_2), progesterone (P), prolactin (PRL), luteinizing hormone (LH), testosterone (T) and human chorionic gonadotropin β (β-HCG)—are shown in Table 1. The PCOS patients showed significantly higher body mass indexes (BMI) and increased levels of luteinizing hormone (LH) compared to normal women ($p < 0.05$). No significant difference was found for other features. The GCs of the above-mentioned PCOS and normal women were then obtained and used for subsequent experiments, as the graphic workflow in Figure 1 showed.

Table 1. Clinical characteristics of polycystic ovarian syndrome (PCOS) and control subjects.

Clinical characteristics	PCOS (n = 14)	Normal (n = 13)	*p* values
Age (years)	29.3±3.89	31.07±4.79	0.293
BMI (kg/m²)	24.82±3.36	21.95±2.58	0.005
W(cm)	75.2±5.59	76.8±6.27	0.596
H(cm)	92±4.92	91.53±5.26	0.166
FSH (mlU/ml)	5.01±1.68	5.28±2.13	0.742
E2(pg/ml)	55.86±44.08	55.67±32.64	0.404
P (ng/ml)	0.78±0.38	0.62±0.2	0.184
PRL (ng/ml)	11.06±6.62	11.31±6.04	0.408
LH (mIU/ml)	7.76±3.88	3.54±2.25	0.004
T(ng/ml)	1.69±0.94	1.54±0.46	0.659
β-HCG (mIU/ml)	0.98±0.55	0.82±0.62	0.217
Fasting glucose (mmol/L)	5.1±0.31	5.11±0.35	0.737

All data are presented as the mean ± SEM. $p < 0.05$ was considered significant. BMI, body mass index; W, waist circumference; H, hip circumference; FSH, follicle stimulating hormone; E2, estrogen; P, progesterone; PRL, prolactin; LH, luteinizing hormone; T, testosterone; β-HCG, human chorionic gonadotropin β.

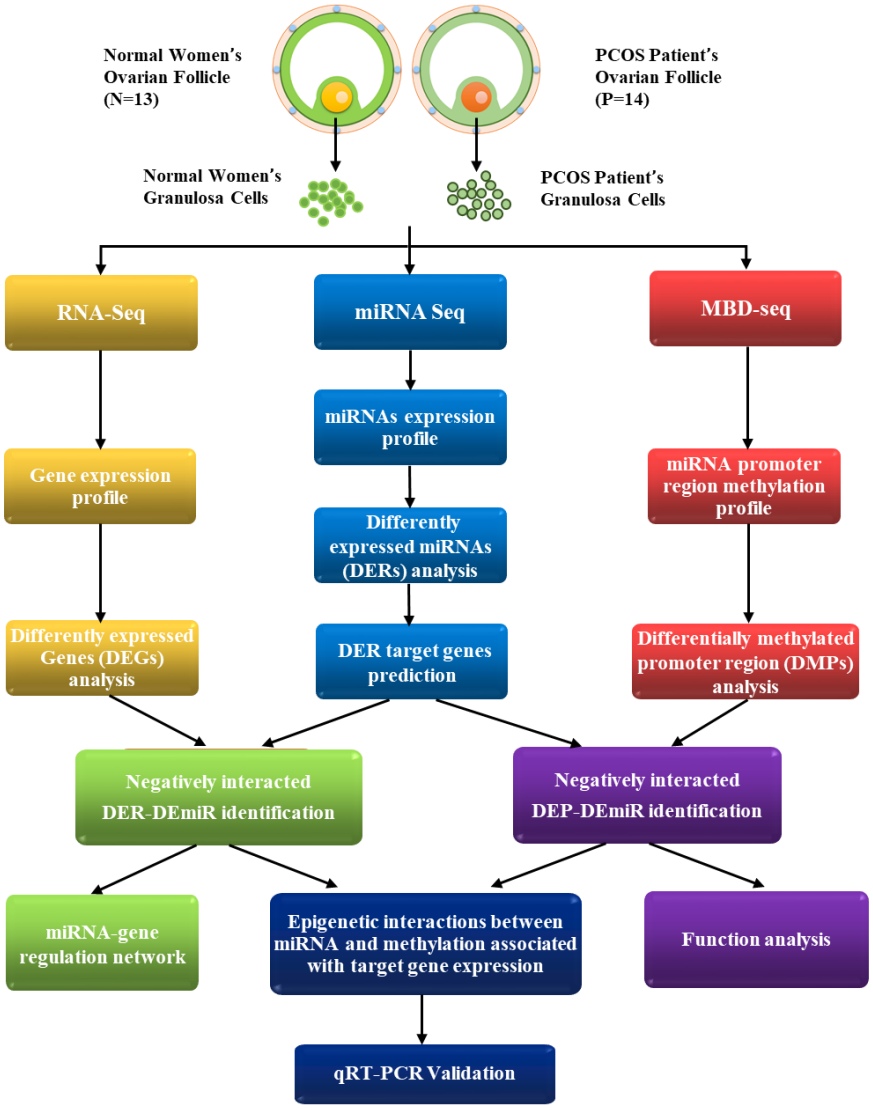

Figure 1. Workflow of experiment and data analysis.

3.2 Identification of DEGs in GCs between PCOS patients and controls

To determine the significant genes in PCOS patients, the transcriptome profiles of GCs from three PCOS and three control women were sequenced and analyzed. Detailed information regarding the sequencing data is summarized in Table S2. In order to better identify DEGs, the intersection of two different identification methods, DESeq2 and edgeR, was used as the final dataset (Table S3). The hierarchical clustering result indicated the significantly different expression patterns between GCs from PCOS and normal women (Fig. 2A). In total, 830 genes were found to be DEGs, including 538 upregulated genes and 292 downregulated genes in PCOS vs. normal GCs (Fig. 2B and 2C). Moreover, we tested the reliability of transcriptome sequencing results by using qRT-PCR, and the results demonstrated a high consistency in the randomly selected five genes' (three upregulated and two downregulated genes) expression between RNA sequencing data and qRT-PCR (Figure 2D).

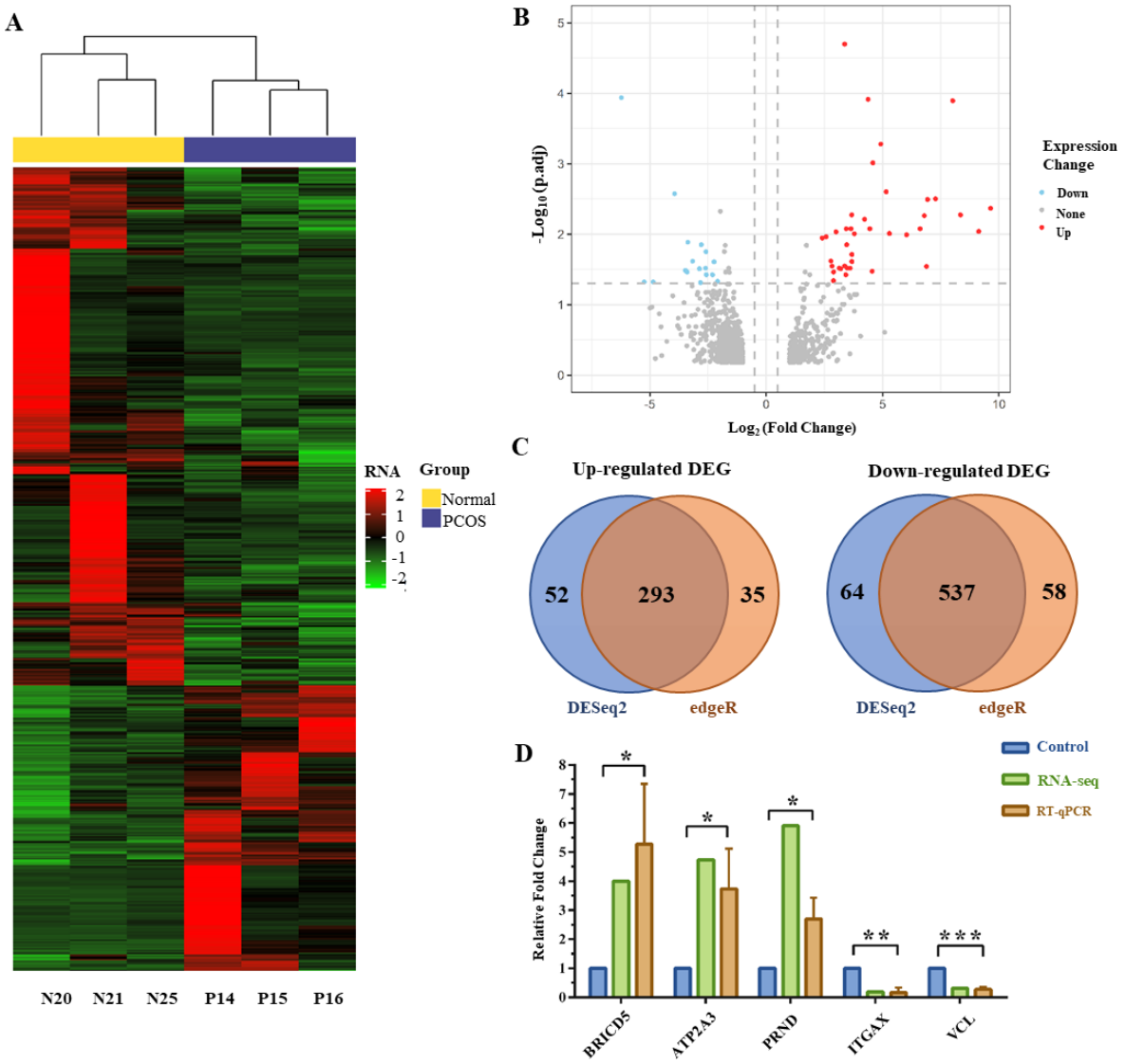

Figure 2. Workflow of experiment and data analysis. Gene expression profile of PCOS vs Normal granulosa cells (GCs) by RNA-seq. (A) Heat map of differentially expressed genes (DEGs) in GCs (P: PCOS GCs; N: Normal GCs); (B) Volcano plot of DEGs in GCs. Upregulated genes are represented by red, and downregulated genes are represented by blue; (C) Venn diagram of identified DEGs in GCs between the DESeq2 method and edgeR method. Results of DESeq2 are shown as blue, and the edgeR method is orange. (D) qRT-PCR validation (*, $0.01 < p < 0.05$; **, $p < 0.01$)

3.3 Identification of DEmiRs in GCs between PCOS patients and controls

Small RNA libraries were constructed to identify miRNA expression differences between the GCs of PCOS and normal women. A total of 23,447,261 and 21,642,858 clean reads which mapped to the genome were acquired from PCOS and normal GCs, respectively (Table S2). We identified 30 significant DEmiRs (Table S4) and performed hierarchical clustering to show the separate miRNA expression patterns between GCs from PCOS and normal women (Figure 3A). Based on the intersection of two different identification methods, eight miRNAs were upregulated and 22 were downregulated significantly in PCOS GCs (Figure 3B and 3C). In addition, the results of small RNA sequencing (three upregulated and two downregulated miRNAs) were validated by qRT-PCR to prove the reliability of this method (Figure 3D).

Then, to characterize the regulatory roles of DEmiRs, the potential miRNA target genes were predicted (Table S5). Among the 312 predicted target genes, *PTEN*, *BCL2*, *HIF1A*, *CDKN1A* and *DNMT1* had the highest count of potential regulatory miRNAs. Moreover, we analyzed the regulatory function of DEmiRs by using the Gene Ontology (GO) database and Kyoto Encyclopedia

Preprints (www.preprints.org) | NOT PEER-REVIEWED | Posted: 17 October 2019 doi:10.20944/preprints201910.0191.v1

Peer-reviewed version available at Journal of Human Genetics 2020; doi:10.1038/s10038-020-0819-6

of Genes and Genomes (KEGG). Certain GO terms were significantly enriched in the biological process, such as cellular response to different stimuli, stress-activated protein kinase signaling cascade (GO: 0031098), stress-activated MAPK cascade (GO: 0051403), hormone response, response to steroid hormone (GO: 0048545), and response to peptide (GO: 1901652) (Figure 3E). In addition, the results of the KEGG analysis indicated that the putative target genes of DEmiRs were involved in the FoxO signaling pathway, the AGE-RAGE signaling pathway in diabetic complications, PI3K-Akt signaling pathway, cellular senescence, and the MAPK signaling pathway (Figure 3F).

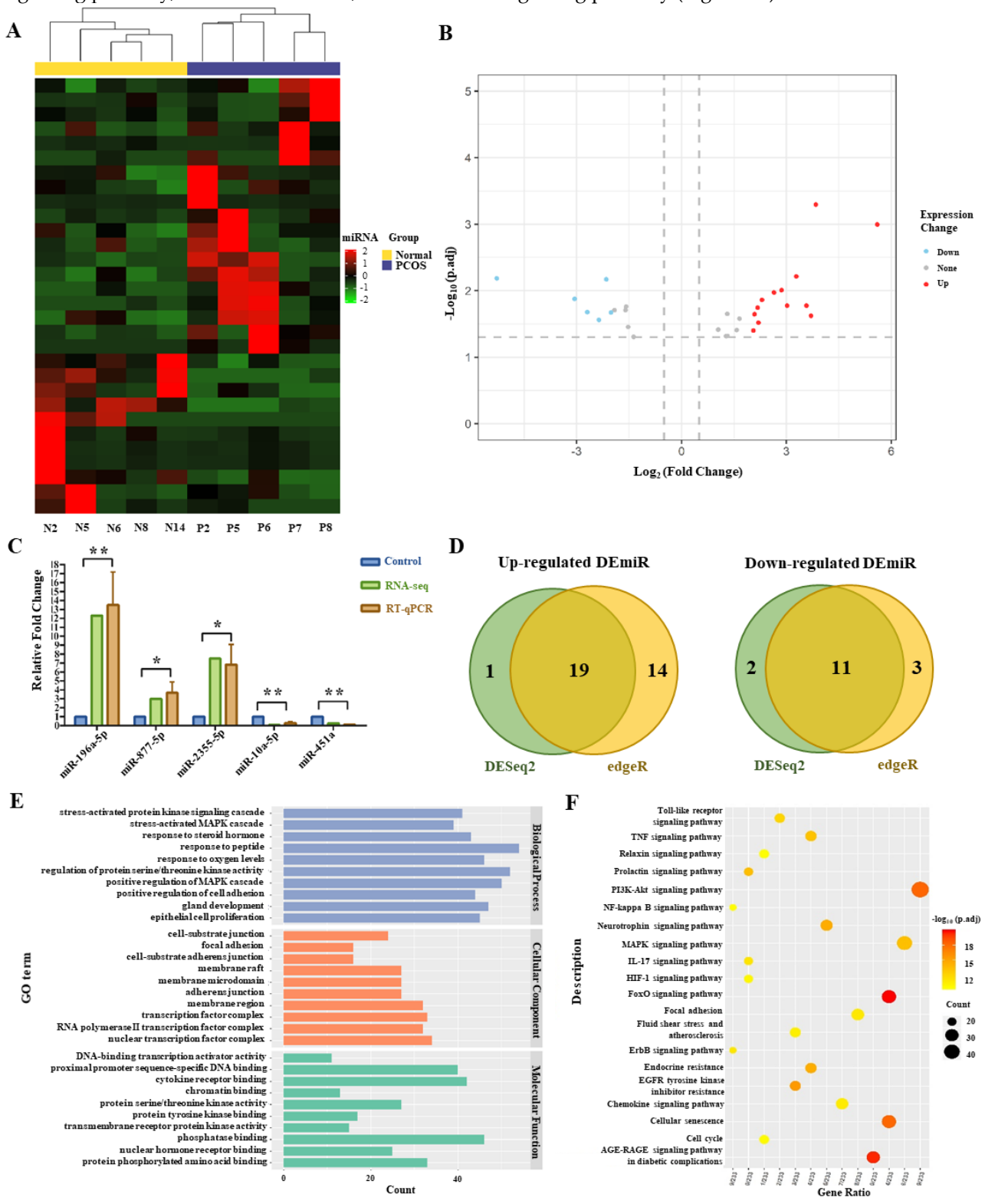

Figure 3. miRNA profile of PCOS vs Normal GCs by small RNA-seq. (A) Heat map of DEmiRs in GCs (P: PCOS GCs; N:Normal GCs); (B) Volcano plot of DEmiRs in GCs. Upregulated miRNAs are

represented by red, and downregulated miRNAs are represented by blue; (C) Venn diagram of identified DEmiRs in GCs between DESeq2 method and edgeR method. Results of DESeq2 are shown as blue, and the edgeR method is orange. (D) (* $0.01<p<0.05$; ** $p<0.01$). (E) Gene Ontology (GO) terms of DEmiRs target genes. (F) Kyoto Encyclopedia of Genes and Genomes (KEGG) analysis of DEmiRs target genes.

3.4 Identification of the DEmiRs that negatively regulated targeted mRNA expression

To illustrate the regulatory functions of the miRNAs in PCOS, we found 10 pairs of miRNA and genes which had a significant negative correlation in expression, respectively, with the identified 830 DEGs and 30 DEmiRs (Table 2). In order to further investigate the role of miRNA–gene pairs in PCOS, a miRNA-gene interaction network was then constructed by Cytoscape (Figure 4). The network consists of six paired miRNA-gene and 47 DEGs genes that were highly aggregated in interaction network. As demonstrated in Figure 4, the DEGs in interaction with each other were associated with several downstream pathways, such as the NOD-like receptor signaling pathway, MAPK signaling pathway, interleukin (IL)-17 signaling pathway, tumor necrosis factor (TNF) signaling pathway, PI3K-Akt signaling pathway, nuclear factor (NF)-kappa B signaling pathway, AGE-RAGE signaling pathway in diabetic complications, Th17 cell differentiation, Toll-like receptor signaling pathway and the chemokine signaling pathway. Furthermore, the upregulation of miR-100-3p and miR-196a-5p was involved in the downstream pathways by inhibiting the expression of respective target genes *CXCL8* and *S100A9*. Additionally, four down-regulated miRNAs participated in the regulation of downstream pathways by reducing the transcription repression of target genes including miR-141-3p/*MAPK14*, miR-144-5/*RUNX1*, miR-18a-5p/*RUNX1* and miR-429/*XIAP*.

Table 2. Negatively regulated miRNA–gene pairs in PCOS.

miRNA	Log_2FC(miRNA)	miRNA Expression change	Target Gene	Log_2FC(Gene)	Gene Expression change
hsa-miR-18a-5p	–2.15	Down	RUNX1	1.47	Up
hsa-miR-100-3p	1.58	Up	CXCL8	–1.45	Down
hsa-miR-126-3p	–1.92	Down	SLC7A5	1.23	Up
hsa-miR-141-3p	–3.06	Down	BRD3	1.56	Up
hsa-miR-141-3p	–3.06	Down	MAPK14	1.36	Up
hsa-miR-144-5p	–2.02	Down	RUNX1	1.47	Up
hsa-miR-196a-5p	3.57	Up	ANXA1	–2.01	Down
hsa-miR-196a-5p	3.57	Up	LSP1	–1.75	Down
hsa-miR-196a-5p	3.57	Up	S100A9	–3.94	Down
hsa-miR-429	–1.60	Down	XIAP	2.20	Up

Log_2FC (miRNA), miRNA expression change between GCs of PCOS patients and normal women (PCOS GCs vs Normal GCs); Log_2FC (Gene), gene expression change between GCs of PCOS patients and normal women (PCOS GCs vs Normal GCs).

Preprints (www.preprints.org) | NOT PEER-REVIEWED | Posted: 17 October 2019 doi:10.20944/preprints201910.0191.v1

Peer-reviewed version available at Journal of Human Genetics 2020; doi:10.1038/s10038-020-0819-6

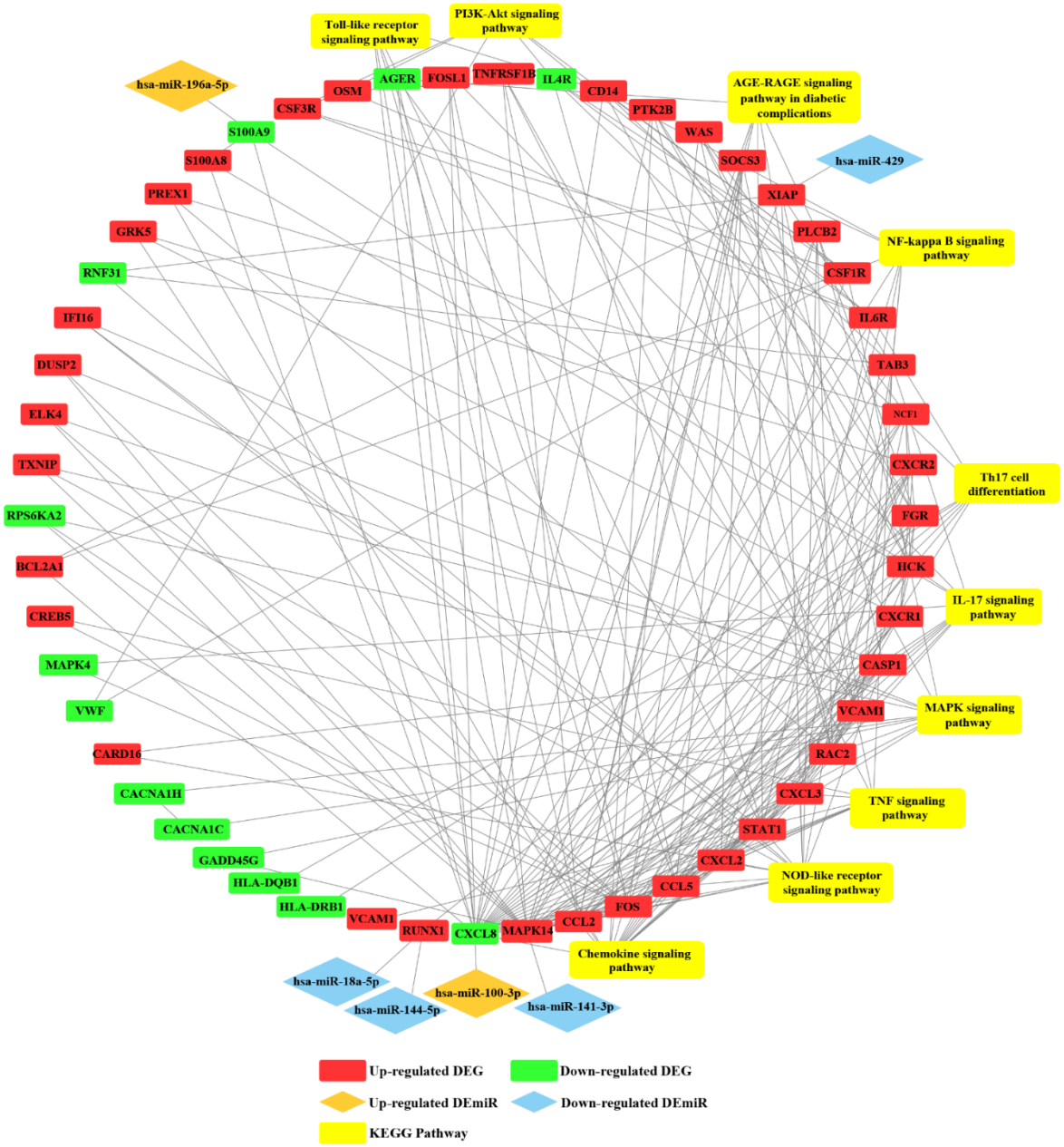

Figure 4. Integrated analysis of DEG–DEmiR pairs (a red diamond represents an upregulated gene; a green diamond represents a downregulated gene; an orange rhombus represents upregulated miRNA; a blue rhombus represents downregulated miRNA; a yellow diamond represents a related KEGG pathway).

3.5 Identification of DEGs in GCs between PCOS patients and controls

Aberrant DNA methylation of the miRNA promoter region directly regulates the expression of miRNA. To determine the global methylation pattern of miRNA promoter region in PCOS, we assessed the methylation levels and genomic distribution of both hypomethylated and hypermethylated miRNA promoter regions of 130 miRNA and found that they were significantly differently methylated (Table S6). As shown in Figure 5A, we observed a significant hypermethylation of global miRNA promoter regions in PCOS GCs, as 10 DMPs (7.69%) were hypomethylated and 120 DMPs (92.3%) were hypermethylated. In addition, the majority of hypermethylated DMPs were found to be located in chromosome 14 and chromosome X.

Then, a function analysis was performed on 719 predicted target genes of the aforementioned 130 miRNAs to understand the biological significance of the miRNAs with hypermethylated promoters in PCOS patients (Table S7). We found that the hypermethylated DEmiRs were mostly

involved in the regulation of cell proliferation, development and stimuli response, such as epithelial cell proliferation (GO: 0050673), gland development (GO: 0048732) and response to peptide (GO: 1901652). Additionally, KEGG analysis results showed over-represented biological processes including the PI3K-Akt signaling pathway, FoxO signaling pathway and MAPK signaling pathway.

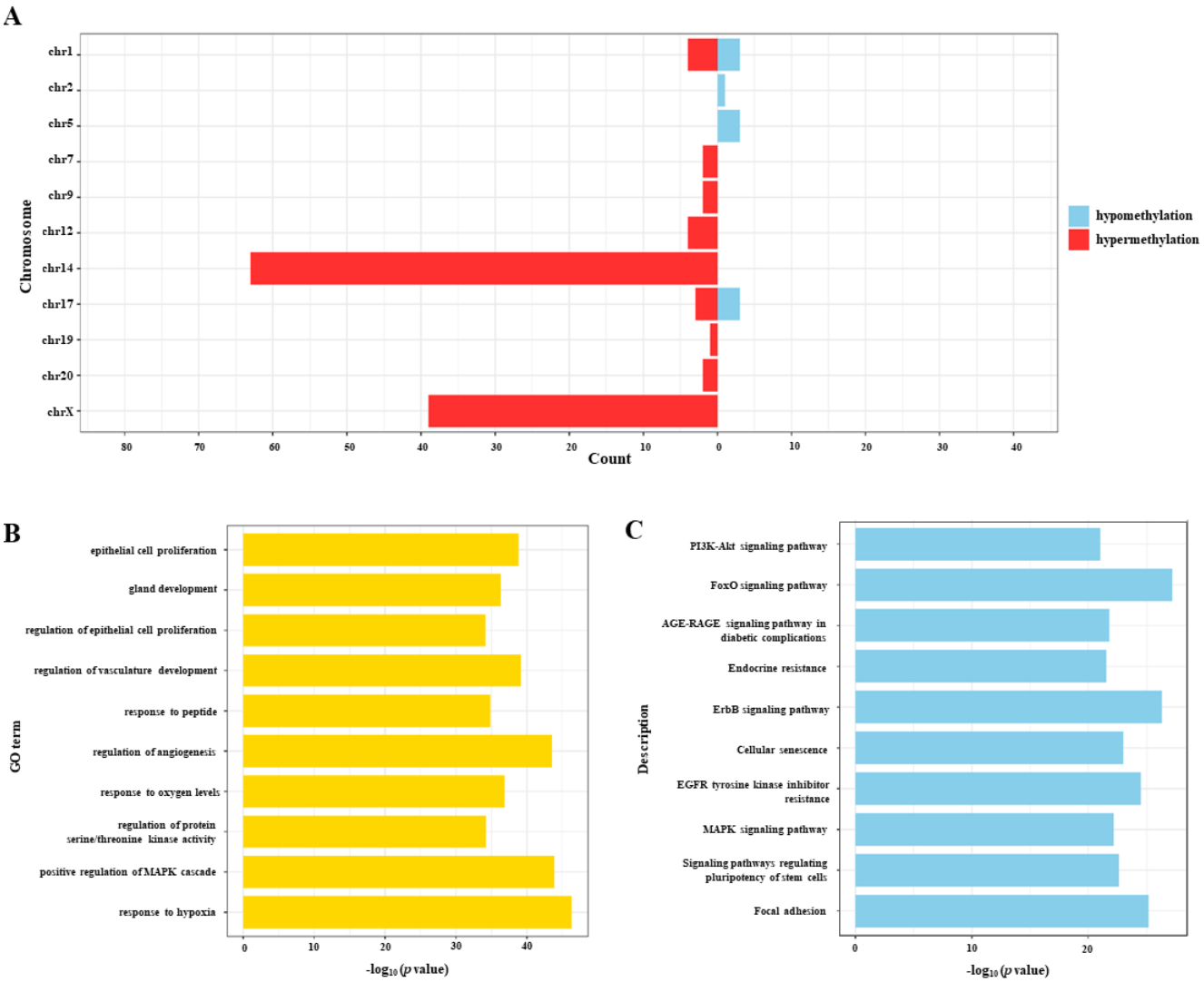

Figure 5. MiRNA promoter region methylation alternation of PCOS vs Normal GCs by methylated DNA binding domain sequencing (MBD-seq). (A) Representation of the distribution of hypomethylated (blue) and hypermethylated (red) regions across genomes. (B) GO terms of promoter hypermethylated miRNA target genes. (C) KEGG analysis of promoter hypermethylated miRNA target genes.

3.6 Identification of DEGs in GCs between PCOS patients and controls

Next, we examined the interactions between miRNA and DNA methylation; 13 miRNA promoter methylation interactions that were significantly associated with expression were identified and are presented in Table 3. To further determine the effect of the interaction between DMPs and DEmiRs on gene expression, we investigated the expression change of promoter aberrant methylated DEmiRs target genes. We found three DEmiRs with DMP were associated with target gene expression levels. As demonstrated in Figure 6A, the promoter region of miR-429, miR-141-3p and miR-126-3p were significantly hypermethylated in PCOS GCs compared to normal controls. Subsequently, we validated the relationship between the three DEmiRs with DMP and their target genes using qRT-PCR (Figure 6B). The expression of miR-429 and its target gene *XIAP* were negatively correlated, while the expression patterns of miR-141-3p and its target genes *BRD3* and *MAPK14* and miR-126-3p and its target gene *SLC7A5* were consistent with what we observed in miR-

429 and *XIAP*. The schematic diagram of interactions between the above-mentioned miRNAs and methylation associated with target gene expression is presented in Figure 6C.

Table 3. The interaction between differentially methylated promoters (DMPs) and DEmiRs in PCOS.

miRNA	Chromosome	Log2FC (miRNA promoter region methylation)	Methylation level change	Log2FC (miRNA)	miRNA Expression change
hsa-miR-216a-5p	chr2	–1.98	–	1.13	Up
hsa-miR-429	chr1	1.57	+	–1.60	Down
hsa-miR-126-3p	chr9	1.10	+	–1.92	Down
hsa-miR-141-3p	chr12	1.36	+	–3.06	Down
hsa-miR-1185-5p	chr14	1.22	+	–2.21	Down
hsa-miR-1197	chr14	1.22	+	–1.24	Down
hsa-miR-412-5p	chr14	1.22	+	–1.23	Down
hsa-miR-431-3p	chr14	1.22	+	–1.26	Down
hsa-miR-431-5p	chr14	1.22	+	–1.16	Down
hsa-miR-433-3p	chr14	1.22	+	–1.37	Down
hsa-miR-485-5p	chr14	1.22	+	–1.02	Down
hsa-miR-487a-3p	chr14	1.22	+	–1.07	Down
hsa-miR-652-5p	chrX	1.21	+	–1.33	Down

Log_2FC (miRNA promoter region methylation), methylation change located in promoter region of miRNAs between GCs of PCOS patients and normal women (PCOS GCs vs Normal GCs); Log_2FC (miRNA), miRNA expression change between GCs of PCOS patients and normal women (PCOS GCs vs Normal GCs); +, hypermethylation; -, hypomethylation.

Preprints (www.preprints.org) | NOT PEER-REVIEWED | Posted: 17 October 2019 doi:10.20944/preprints201910.0191.v1

Peer-reviewed version available at Journal of Human Genetics 2020; doi:10.1038/s10038-020-0819-6

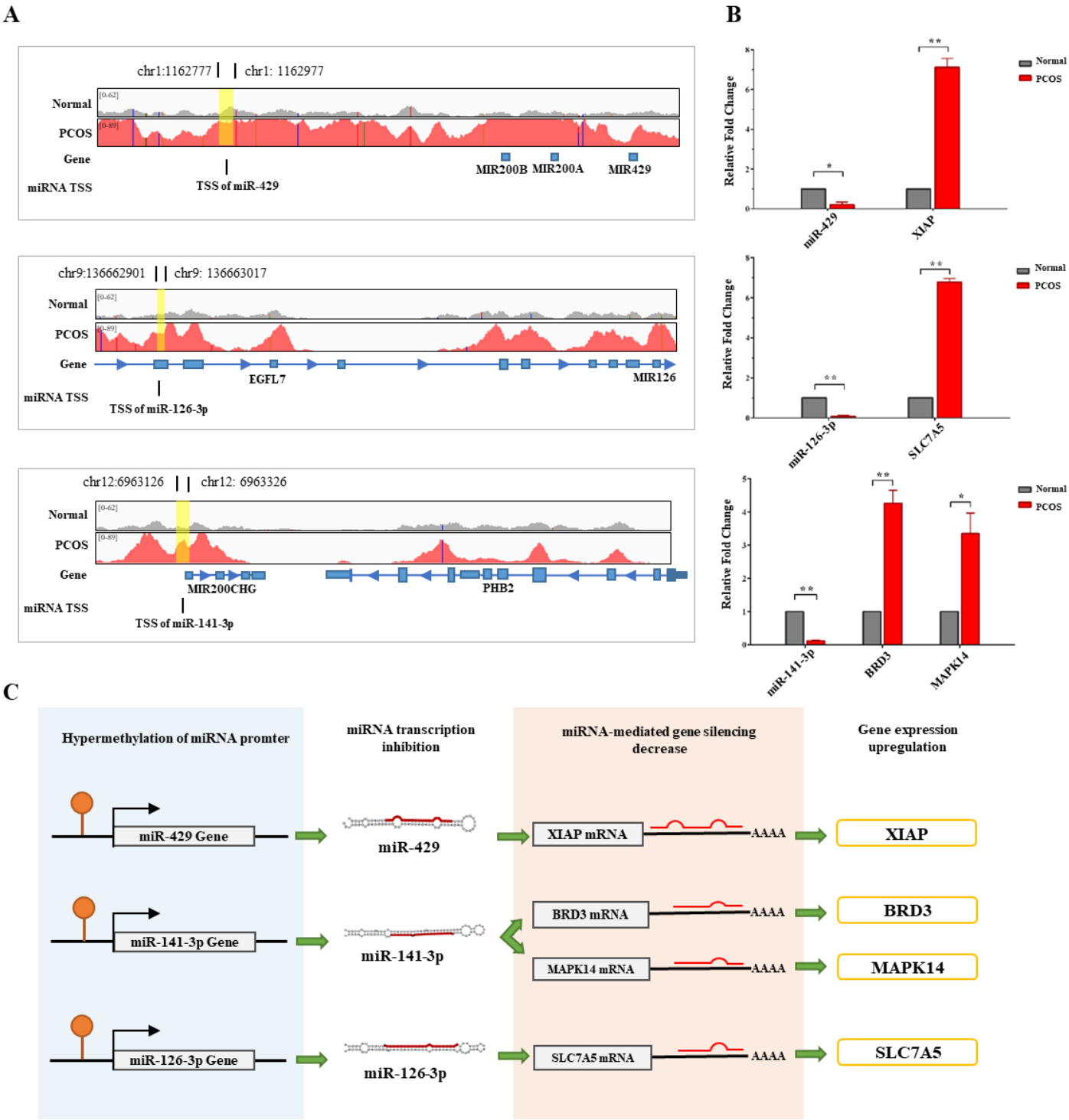

Figure 6. The hypermethylation of miRNA promoters leads to miRNA silencing and the disinhibition of target genes. (A) A signal view of miR-429, miR-141-3p and miR-126-3p promoter region methylation in GCs of PCOS (red) and control (grey) groups. (B) Expression changes of miR-429, miR-141-3p and miR-126-3p and target genes were verified by RT-qPCR. (C) Schematic diagram of interactions between miRNAs and methylation associated with target gene expression.

4. Discussion

Epigenetic modification regulates gene expression during multiple critical physiological and pathological processes, including cell proliferation, apoptosis, inflammation and carcinogenesis. Among all the epigenetic modifications, DNA methylation and miRNA are both major epigenetic regulators that are reportedly involved in the development of PCOS. Moreover, DNA methylation and miRNA interact with each other and, along with other epigenetic mechanisms, govern the gene

expression levels of mRNA and proteins. However, the epigenetic interaction between miRNA and DNA methylation associated with mRNA transcription in PCOS remains unreported.

In the present study, we performed RNA-seq and found 830 DEGs in GCs of PCOS patients, with 538 (64.82%) upregulated and 292 (35.18%) downregulated (Figure 2). Using small RNA sequencing, 30 DEmiRs was identified, including eight (26.67%) upregulated and 22 (73.33%) downregulated miRNAs, and 312 target genes of DEmiRs were predicted using the miRTarbase database (Figure 3). The GO terms of DEmiRs target genes were significantly enriched in biological processes such as cellular response to different stimuli, the cascade of stress-activated protein kinase (SAPK), and mitogen-activated protein kinase (MAPK), which participate in modulating processes such as inflammation and immune activation, development, and apoptosis [28,29].

Moreover, among the 312 predicted corresponding genes, 22 were identified as significantly differentially expressed based on transcriptome profiles, and the expression of nine genes was negatively regulated by seven miRNAs (Table 2). For example, there was a negative correlation between miR-141-3p (downregulation) and two genes, *BRD3* (upregulation) and *MAPK14* (upregulation), respectively. Also, there were two miRNAs, miR-144-5p (downregulation) and miR-18a-5p (downregulation), targeting the same gene, *RUNX1* (upregulation), in PCOS. To further illustrate the regulatory functions of negatively regulated PCOS-related DEGs and DEmiRs, we constructed a PPI network with Cytoscape (Figure 4). The results illustrated that miR-100-3p (upregulation)/ *CXCL8* (downregulation), miR-196a-5p (upregulation)/ *S100A9* (downregulation), miR-141-3p (downregulation)/ *MAPK14* (upregulation), miR-144-5 (downregulation)/ *RUNX1* (upregulation), miR-18a-5p (downregulation)/ *RUNX1* (upregulation) and miR-429 (downregulation)/ *XIAP* (upregulation) compactly participated in the regulation network consisting of 53 identified DEGs. Therefore, these were associated with the NOD-like receptor signaling pathway, MAPK signaling pathway, IL-17 signaling pathway, TNF signaling pathway, PI3K-Akt signaling pathway, NF-kappa B signaling pathway, AGE-RAGE signaling pathway in diabetic complications, Th17 cell differentiation, Toll-like receptor signaling pathway, and chemokine signaling pathway. Among these, the MAPK signaling pathway [30], PI3K-Akt signaling pathway [31], and Toll-like receptor signaling pathway [32] had been reported to be involved in PCOS previously by performing apoptosis and cell-proliferation related processes.

Furthermore, we performed MBD-seq to characterize the miRNA promoter methylation pattern in PCOS GCs. Compared to normal women, the majority of DMPs in PCOS were hypermethylated (92.3%) and mainly located in chromosome 14 (48.46%) and chromosome X (30%). In various species, the miRNA distribution pattern is uneven, with miRNA concentrated into certain chromosomes and physically adjacent miRNA genes transcribed as clusters [33]. A previous study reported that certain chromosomes have relatively higher counts of miRNA associated with development and disease processes, such as chromosomes 1, 14, 19, and X [34]. In our study, we found 63 miRNAs with DMPs that are members of the human chromosome 14 microRNA cluster (C14MC), which was reported to control important biological functions in placental and embryonic development [35]. Surprisingly, all aforementioned members of C14MC shared the same hypermethylated promoter region, which is consistent with another study which showed that multiple pre-miRNA transcripts may be produced from the same pre-miRNA cluster. In contrast, the 39 miRNAs localized in chromosome X corresponded to nine different hypermethylated promoter regions (Table S6). These observations suggest that underlying epigenetic mechanisms may play an important role in the chromosome 14 and chromosome X-regulated cellular processes in PCOS.

DNA methylation can result in the inhibition of miRNA transcription by hypermethylating the CpG islands in the promoter regions of miRNAs. In this study, we found 12 miRNA silencing events caused by the hypermethylation of the miRNA-coding gene promoter, and one hypomethylation of a miRNA promoter led to its upregulation. Additionally, the DNA methylation of the miRNA promoter region controlling its corresponding gene expression was observed in miR-429, miR-141-3p and miR-126-3p. All four target genes of these miRNAs, *XIAP*, *BRD3*, *MAPK14* and *SLC7A5*, were upregulated due to the reduced suppression of miRNA, which is caused by its transcription inhibition resulting from promoter hypermethylation (Figure 6).

MAPK14 and miR-141-3p have both been identified as being related to PCOS. The coding protein of *MAPK14* is a member of the mitogen-activated protein (MAP) kinase family and is involved in serval critical biological processes such as cell proliferation, differentiation, and development [29]. Cabergoline (Cb2), one of the dopamine receptor 2 agonists, has been used to reduce the ovarian hyperstimulation risk associated with PCOS, and *MAPK14* was shown to be a key gene implicated in these pathways in Cb2 response, which might be a potential biomarker for further studies of PCOS [36]. *MAPK14* was also found to participate in the biosynthesis of human androgen, a hormone whose excessive production was mainly induced by PCOS [37]. Likewise, the differential expression of miR-141-3p was reported in rat models of PCOS induced by letrozole, and consistently with our findings, it showed a significantly decreased expression in the PCOS group and regulated the MAPK signaling pathway [38]. Our study further demonstrated the complicated epigenetic mechanism underlying miR-141-3p/*MAPK14* regulation in GC function.

In addition, previous studies have also suggested that *XIAP* and miR-429 are involved in the mechanism of cell apoptosis and anovulation, respectively. Most of the GCs of polycystic ovaries had fundamental and significant differences in the rate of cell death and proliferation and were demonstrated to be more non-apoptotic than GCs of normal follicles [39]. It had previously been reported in another study that the X-linked inhibitor of the apoptosis protein encoded by *XIAP* was involved in blocking apoptosis by inhibiting caspase-3 activity, and the overexpression of *XIAP* has been reported in many diseases such as leukemia and breast cancer [40,41]. On the other hand, miR-429 was found to play an essential role in mammal ovulation. The knockout of miR-429 led to increased *ZEB1* expression in the pituitary of mice, resulting in unsuccessful ovulation [42]. Our results suggested roles for miR-429 and its target gene *XIAP* in the regulation of the GCs of PCOS. Further investigation is needed to determine their specifically regulatory function and potential as biological markers in PCOS.

DNA methylation can result in the inhibition or activation of miRNA transcription by hypermethylating or hypomethylating the CpG islands in the promoter regions of miRNAs. Conversely, miRNAs can also regulate DNA methylation by directly targeting DNA methyltransferases and methylation-related critical proteins, thereby affecting the whole genome methylation pattern [14]. It is worth noting that *DNMT1* was predicted to be a target gene of three DEmiRs including miR-126-3p, miR-18a-5p and miR-429. However, the expression data of *DNMT1* were not found in our transcriptome profile. It is worth further exploring this to confirm the regulation mechanism of DNA methylation by miRNAs in PCOS.

Previous works had proved that individual epigenetic regulation, especially miRNAs and DNA methylation, played an important role in PCOS. Further investigation of DNA methylation patterns and miRNA expression profiles in PCOS will facilitate the foundation of novel therapeutic strategies and the characterization of suitable diagnostic and prognostic markers. The regulatory roles of epigenetic interactions between miRNA and DNA methylation also require deeper exploration to help improve the understanding of the regulation function of GCs in PCOS.

5. Conclusions

In conclusion, in this study, we investigated the relevant dysregulation of miRNA expression and methylation in GCs of PCOS. We confirmed that DNA methylation regulated miRNA transcription by hypermethylating the CpG islands in the promoter regions of miRNAs. Moreover, our results indicated that, by suppressing miRNA, DNA hypermethylation inducing the overexpression of miRNA target genes was found in miR-429/*XIAP*, miR-141-3p/*BRD3*, miR-141-3p/*MAPK14*, and miR-126-3p/*SLC7A5*. The reactivation of the transcription of epigenetically silenced genes may be one of the key elements of PCOS pathogenesis, and the epigenetic mechanisms underlying the regulation of miRNA expression can provide a potential therapeutic target for PCOS in the future.

Supplementary Materials: Table S1: Primer Sequence, Table S2: Sequencing data information, Table S3: Differentially expressed genes, Table S4: Differentially expressed miRNAs, Table S5: Predicted target genes of

DEmiRs, Table S6: Differential methylation of miRNA promoter regions, Table S7: Predicted target genes of miRNAs with DMPs.

Author Contributions: Conceptualization, Z.M. and Y.K.; investigation, Z.M.; software, H.Z.; validation, Z.M. and Y.Q.; material and follow-up data collection and resources, T.L.; writing—original draft preparation, Z.M.; writing—review and editing, Y.K, Y.Q. and H.Z.; visualization, Z.M., Y.Q. and H.Z.; supervision, Y.K.; project administration, Y.K.; funding acquisition, Y.K.

Funding: This work was supported by the Natural Science Foundation of Shanghai (19ZR1476100), Medical Engineering Cross Fund (YG2019GD02, YG2019QNB23, YG2019QNA49 and YG2019QNA52) and Laboratory Innovative Research Program of Shanghai Jiao Tong University (JCZXSJB2019002).

Conflicts of Interest: The authors declare no conflict of interest.

References

1. Franks, S. Polycystic ovary syndrome. *NEW ENGL J MED* **1995**, 333, 853-861.
2. Azziz, R.; Woods, K.S.; Reyna, R.; Key, T.J.; Knochenhauer, E.S.; Yildiz, B.O. The Prevalence and Features of the Polycystic Ovary Syndrome in an Unselected Population. *The Journal of Clinical Endocrinology & Metabolism* **2004**, 89, 2745-2749.
3. Norman, R.J.; Dewailly, D.; Legro, R.S.; Hickey, T.E. Polycystic ovary syndrome. *LANCET* **2007**, 370, 685-697.
4. Matsuda, F.; Inoue, N.; Manabe, N.; Ohkura, S. Follicular growth and atresia in mammalian ovaries: regulation by survival and death of granulosa cells. *J Reprod Dev* **2012**, 58, 44-50.
5. Das, M.; Djahanbakhch, O.; Hacihanefioglu, B.; Saridogan, E.; Ikram, M.; Ghali, L.; Raveendran, M.; Storey, A. Granulosa Cell Survival and Proliferation Are Altered in Polycystic Ovary Syndrome. *The Journal of Clinical Endocrinology & Metabolism* **2008**, 93, 881-887.
6. Li, S.; Zhu, D.; Duan, H.; Tan, Q. The epigenomics of polycystic ovarian syndrome: from pathogenesis to clinical manifestations. *GYNECOL ENDOCRINOL* **2016**, 32, 942-946.
7. Holubekova, V.; Mendelova, A.; Jasek, K.; Mersakova, S.; Zubor, P.; Lasabova, Z. Epigenetic regulation by DNA methylation and miRNA molecules in cancer. *FUTURE ONCOL* **2017**, 13, 2217-2222.
8. Yu, Y.; Sun, C.; Liu, Y.; Li, Y.; Wang, L.; Zhang, W. Genome-wide screen of ovary-specific DNA methylation in polycystic ovary syndrome. *FERTIL STERIL* **2015**, 104, 145-153.
9. Kokosar, M.; Benrick, A.; Perfilyev, A.; Fornes, R.; Nilsson, E.; Maliqueo, M.; Behre, C.J.; Sazonova, A.; Ohlsson, C.; Ling, C.; et al. Epigenetic and Transcriptional Alterations in Human Adipose Tissue of Polycystic Ovary Syndrome. *SCI REP-UK* **2016**, 6.
10. Xu, J.; Bao, X.; Peng, Z.; Wang, L.; Du, L.; Niu, W.; Sun, Y. Comprehensive analysis of genome-wide DNA methylation across human polycystic ovary syndrome ovary granulosa cell. *Oncotarget* **2016**, 7, 27899-27909.
11. Tu, J.; Cheung, A.H.; Chan, C.L.; Chan, W. The Role of microRNAs in Ovarian Granulosa Cells in Health and Disease. *FRONT ENDOCRINOL* **2019**, 10.
12. Chen, B.; Xu, P.; Wang, J.; Zhang, C. The role of MiRNA in polycystic ovary syndrome (PCOS). *GENE* **2019**, 706, 91-96.
13. Chhabra, R. miRNA and Methylation: A Multifaceted Liaison. *CHEMBIOCHEM* **2015**, 16, 195-203.
14. Wang, S.; Wu, W.; Claret, F.X. Mutual regulation of microRNAs and DNA methylation in human cancers. *EPIGENETICS-US* **2017**, 12, 187-197.
15. Revised 2003 consensus on diagnostic criteria and long-term health risks related to polycystic ovary syndrome (PCOS). *HUM REPROD* **2004**, 19, 41-47.
16. Kim, D.; Paggi, J.M.; Park, C.; Bennett, C.; Salzberg, S.L. Graph-based genome alignment and genotyping with HISAT2 and HISAT-genotype. *NAT BIOTECHNOL* **2019**, 37, 907-915.
17. Pertea, M.; Kim, D.; Pertea, G.M.; Leek, J.T.; Salzberg, S.L. Transcript-level expression analysis of RNA-seq experiments with HISAT, StringTie and Ballgown. *NAT PROTOC* **2016**, 11, 1650-1667.
18. Love, M.I.; Huber, W.; Anders, S. Moderated estimation of fold change and dispersion for RNA-seq data with DESeq2. *GENOME BIOL* **2014**, 15.
19. Robinson, M.D.; McCarthy, D.J.; Smyth, G.K. edgeR: a Bioconductor package for differential expression analysis of digital gene expression data. *BIOINFORMATICS* **2009**, 26, 139-140.
20. Langmead, B.; Salzberg, S.L. Fast gapped-read alignment with Bowtie 2. *NAT METHODS* **2012**, 9, 357-359.
21. Kozomara, A.; Birgaoanu, M.; Griffiths-Jones, S. miRBase: from microRNA sequences to function. *NUCLEIC ACIDS RES* **2019**, 47, D155-D162.

22. Chou, C.; Shrestha, S.; Yang, C.; Chang, N.; Lin, Y.; Liao, K.; Huang, W.; Sun, T.; Tu, S.; Lee, W.; et al. miRTarBase update 2018: a resource for experimentally validated microRNA-target interactions. *NUCLEIC ACIDS RES* **2018**, 46, D296-D302.
23. Yu, G.; Wang, L.; Han, Y.; He, Q. clusterProfiler: an R Package for Comparing Biological Themes Among Gene Clusters. *OMICS: A Journal of Integrative Biology* **2012**, 16, 284-287.
24. Szklarczyk, D.; Franceschini, A.; Wyder, S.; Forslund, K.; Heller, D.; Huerta-Cepas, J.; Simonovic, M.; Roth, A.; Santos, A.; Tsafou, K.P.; et al. STRING v10: protein–protein interaction networks, integrated over the tree of life. *NUCLEIC ACIDS RES* **2015**, 43, D447-D452.
25. Shannon, P.; Markiel, A.; Ozier, O.; Baliga, N.S.; Wang, J.T.; Ramage, D.; Amin, N.; Schwikowski, B.; Ideker, T. Cytoscape: a software environment for integrated models of biomolecular interaction networks. *GENOME RES* **2003**, 13, 2498-2504.
26. Lienhard, M.; Grimm, C.; Morkel, M.; Herwig, R.; Chavez, L. MEDIPS: genome-wide differential coverage analysis of sequencing data derived from DNA enrichment experiments. *BIOINFORMATICS* **2014**, 30, 284-286.
27. Lizio, M.; Abugessaisa, I.; Noguchi, S.; Kondo, A.; Hasegawa, A.; Hon, C.C.; de Hoon, M.; Severin, J.; Oki, S.; Hayashizaki, Y.; et al. Update of the FANTOM web resource: expansion to provide additional transcriptome atlases. *NUCLEIC ACIDS RES* **2019**, 47, D752-D758.
28. Tibbles, L.A.; Woodgett, J.R. The stress-activated protein kinase pathways. *CELL MOL LIFE SCI* **1999**, 55, 1230-1254.
29. LiuHT, Z. MAPK signal pathways in the regulation of cell proliferation in mammalian cells. *Cell Research* **2002**, 12, 9-18.
30. Aydos, A.; Gurel, A.; Oztemur Islakoglu, Y.; Noyan, S.; Gokce, B.; Ecemis, T.; Kaya, C.; Aksu, A.T.; Gur Dedeoglu, B. Identification of Polycystic Ovary Syndrome (PCOS) Specific Genes in Cumulus and Mural Granulosa Cells. *PLOS ONE* **2016**, 11, e168875.
31. Zhao, H.; Zhou, D.; Chen, Y.; Liu, D.; Chu, S.; Zhang, S. Beneficial effects of Heqi san on rat model of polycystic ovary syndrome through the PI3K/AKT pathway. *DARU* **2017**, 25, 21.
32. Bi, X.; Zhai, Z.; Wang, S. Identification of the key pathways and genes related to polycystic ovary syndrome using bioinformatics analysis. *GEN PHYSIOL BIOPHYS* **2019**, 38, 205-2014.
33. Chan, W.; Ho, M.; Li, S.; Tsai, K.; Lai, C.; Hsu, C.; Lin, W. MetaMirClust: Discovery of miRNA cluster patterns using a data-mining approach. *GENOMICS* **2012**, 100, 141-148.
34. Ghorai, A.; Ghosh, U. miRNA gene counts in chromosomes vary widely in a species and biogenesis of miRNA largely depends on transcription or post-transcriptional processing of coding genes. *FRONT GENET* **2014**, 5.
35. Dini, P.; Daels, P.; Loux, S.C.; Esteller-Vico, A.; Carossino, M.; Scoggin, K.E.; Ball, B.A. Kinetics of the chromosome 14 microRNA cluster ortholog and its potential role during placental development in the pregnant mare. *BMC GENOMICS* **2018**, 19.
36. Ferrero, H.; Díaz-Gimeno, P.; Sebastián-León, P.; Faus, A.; Gómez, R.; Pellicer, A. Dysregulated genes and their functional pathways in luteinized granulosa cells from PCOS patients after cabergoline treatment. *REPRODUCTION* **2018**, 155, 373-381.
37. Udhane, S.S.; Flück, C.E. Regulation of human (adrenal) androgen biosynthesis—New insights from novel throughput technology studies. *BIOCHEM PHARMACOL* **2016**, 102, 20-33.
38. Li, D.; Li, C.; Xu, Y.; Xu, D.; Li, H.; Gao, L.; Chen, S.; Fu, L.; Xu, X.; Liu, Y.; et al. Differential Expression of microRNAs in the Ovaries from Letrozole-Induced Rat Model of Polycystic Ovary Syndrome. *DNA CELL BIOL* **2016**, 35, 177-183.
39. Das, M.; Djahanbakhch, O.; Hacihanefioglu, B.; Saridogan, E.; Ikram, M.; Ghali, L.; Raveendran, M.; Storey, A. Granulosa Cell Survival and Proliferation Are Altered in Polycystic Ovary Syndrome. *The Journal of Clinical Endocrinology & Metabolism* **2008**, 93, 881-887.
40. Saraei, R.; Soleimani, M.; Movassaghpour Akbari, A.A.; Farshdousti Hagh, M.; Hassanzadeh, A.; Solali, S. The role of XIAP in resistance to TNF-related apoptosis-inducing ligand (TRAIL) in Leukemia. *BIOMED PHARMACOTHER* **2018**, 107, 1010-1019.
41. Hussain, A.R.; Siraj, A.K.; Ahmed, M.; Bu, R.; Pratheeshkumar, P.; Alrashed, A.M.; Qadri, Z.; Ajarim, D.; Al-Dayel, F.; Beg, S.; et al. XIAP over-expression is an independent poor prognostic marker in Middle Eastern breast cancer and can be targeted to induce efficient apoptosis. *BMC CANCER* **2017**, 17.
42. Hasuwa, H.; Ueda, J.; Ikawa, M.; Okabe, M. MiR-200b and miR-429 Function in Mouse Ovulation and Are Essential for Female Fertility. *SCIENCE* **2013**, 341, 71-73.